View metadata, citation and similar papers at core.ac.uk
brought to you by CORE
provided by RERO DOC Digital Library

Published in "Polymer Chemistry 10(16): 2057–2063, 2019"
which should be cited to refer to this work.

Synthesis and properties of poly(norbornene)s with lateral aramid groups†

Phally Kong,‡[a] Susanne Drechsler,‡[a] Sandor Balog,[b] Stephen Schrettl,[b] Christoph Weder[b] and Andreas F. M. Kilbinger*[a]

This paper deals with the synthesis and investigation of comb-like poly(norbornene)s carrying lateral rod-like aramid groups. Two types of norbornene-based monomers were synthesized and copolymerized with a norbornene carrying an aliphatic side chain using ring opening metathesis polymerization (ROMP). The new monomers contain aramid derivatives that display different types of non-covalent interactions. The first monomer contains linear tri(*p*-benzamide)s, which exhibit the typical H-bonds that aramids are known for. The second monomer features tri(*p*-benzamide)s with bulky ethylhexyloxy side-chains, which suppress intermolecular hydrogen bonding and favor π–π-stacking. The monomers were copolymerized in various ratios and the influence of the composition on the material properties was investigated using Differential Scanning Calorimetry (DSC), Thermogravimetric Analysis (TGA), Dynamic Mechanical Analysis (DMA), and powder X-ray diffraction (XRD) experiments. The results show that the glass transition temperature increases proportionally with the concentration of the H-bonding monomer.

http://doc.rero.ch

Introduction

Aramids are known to be very resistant materials and are known under tradenames such as Kevlar® and Nomex®. The high stiffness of these materials is a result of non-covalent interactions, such as H-bonds.[1–3] Responsible for the attractive material properties on the one side, these interactions also cause drawbacks such as poor solubility and hence processability.[4] One possibility to overcome this disadvantage is the attachment to soluble polymer chains.[5,6] To date, research within the field of comb polymers focused mostly on rod-like polymers with hairy side chains[7,8] or on rigid rod-like side chains connected *via* a flexible linker to the main chain.[9] Only few reports exist on theoretical studies[10] and syntheses[11] of polymers in which the rod-like side chain is directly bound to the main chain. Furthermore, these reports mainly focused on using terephthalic acid, polyphenyl, or phenyl alkynyl oligomers as rigid rods.[12,13] The aim of this work was the synthesis of comb-like poly(norbornene)s carrying lateral rod-like aramid groups and the investigation of how the properties of such materials can be controlled by exploiting different types of non-covalent interactions, which are a powerful tool for supramolecular organization. In this paper, we present the synthesis of statistical copolymers made from norbornene-based monomers carrying either tri(*p*-benzamide) rods or aliphatic side chains. These comb-like polymers were prepared *via* ring-opening metathesis polymerization (ROMP). Aramids are good candidates to undergo different supramolecular interactions, such as hydrogen bonds[14] and aromatic stacking[15,16] In order to investigate the distinct influence of either one of these intermolecular forces, we synthesized two types of monomers containing different rigid rod-like components. One monomer possesses a rod consisting of an aramid trimer able to interact primarily *via* hydrogen bonds. In contrast, the second monomer contains a rigid element, through which π-interactions are more likely to occur. The monomers were copolymerized in various ratios and the influence of the composition on the mechanical and thermal properties was investigated. It was found that hydrogen bonding between the side chains increased the glass transition temperature significantly. Furthermore, it was observed that these interactions were also beneficial for the mechanical properties, resulting in polymers with a higher storage modulus. The findings of this study might serve as blueprints to improve the properties of other polymeric systems.

[a]*University of Fribourg, Chemistry Department, Rue du Musée 9, 1700 Fribourg, Switzerland. E-mail: andreas.kilbinger@unifr.ch*
[b]*Adolphe Merkle Institute, University of Fribourg, Chemin des Verdiers 4, 1700 Fribourg, Switzerland*

†Electronic supplementary information (ESI) available: Syntheses, NMR spectra verifying DMB-deprotection, DLS data, GPC data, NMR calculating actual molar ratio of rod content, complete DSC curves, complete tensile stress-strain-test data and POM photographs. See DOI: 10.1039/c9py00187e

‡These authors contributed equally.

http://doc.rero.ch

Results and discussion

The monomer synthesis started with the thermal conversion of commercially available *cis*-5-norbornene-*endo*-2,3-dicarboxylic anhydride to the *exo*-form. Subsequent reaction with 2-ethyl-1-hexylamine afforded the monomer **EHNI**, which was used for the synthesis of the reference polymer **polEHNI** and as comonomer for the rod-containing statistical copolymers.

The synthesis of the first aramid-carrying monomer with a solubilizing alkyl chain attached to the aramid segment started with the protection of the carboxylic acid of 4-aminosalicylic acid as a methyl ester, which afforded compound **1** (Scheme 1). A 2-ethylhexyl side chain was introduced *via* Williamson ether synthesis between the aromatic hydroxyl group and a haloalkane to give **2**. After saponification of methyl ester **2** into the free carboxylic acid **3**, a condensation with *cis*-5-norbornene-*exo*-2,3-dicarboxylic anhydride yielded the imide **4**. This was followed by consecutive amide bond formations using thionyl chloride in *N*-methyl-2-pyrrolidone (NMP) solution to afford **monoEtHexROD** (Scheme 1). Due to intramolecular hydrogen bond formation between the amide N–H donor and the alkyloxy O-acceptor, no intermolecular aggregation of this trimer *via* hydrogen bonds is possible. However, the intramolecular hydrogen bond formation allows neighbouring phenyl rings to be perfectly coplanar, thereby "flattening" the trimer and allowing greater dispersion force induced stabilization due to the flat rigid shape.[17]

The second aramid-carrying monomer, designed to be able to undergo H-bonding, needed a solubilizing feature to facilitate its synthesis. Thus, in order to prevent H-bonds during synthesis and enable good solubility in non-polar solvents, an *N*-dimethoxybenzyl (DMB) protecting group was attached to the amide linkage, which changes the configuration of the amide bond from *trans* into *cis* (with respect to the phenyl rings). The synthesis started with the methylation of 4-aminobenzoic acid to afford methyl ester **6** (Scheme 2), which was reacted with 2,4-dimethoxybenzaldehyde to afford the secondary amine **7** through reductive amination. Subsequent saponification gave the free carboxylic acid **8**. Finally, the aramid units were consecutively attached in the same manner as for **monoEtHexROD** (Scheme 1) to yield monomer **monoDMBrod** (Scheme 2).

The polymerizations were carried out by fast injection of a degassed dichloromethane (DCM) solution of initiator **G1** (Grubbs' 1st generation catalyst, dichloro(benzylidene)-bis (tricyclohexylphosphine)ruthenium(II)) to a degassed DCM solution of either a mixture of monomers **EHNI** and **monoEtHexROD** (Scheme 3) or a mixture of **ENHI** and **monoDMBrod** (Scheme 4). In both series, the composition was systematically varied and the fraction of the rod-containing monomers was chosen to be 10, 25, 35 and 50 molar percent. The rod percentages are reported in the polymer acronym as P10, P20, P35, and P50 respectively, while the polymers with different type of rod are named according to their rod monomer such as **polEtHexROD** and **polDMBrod**, which

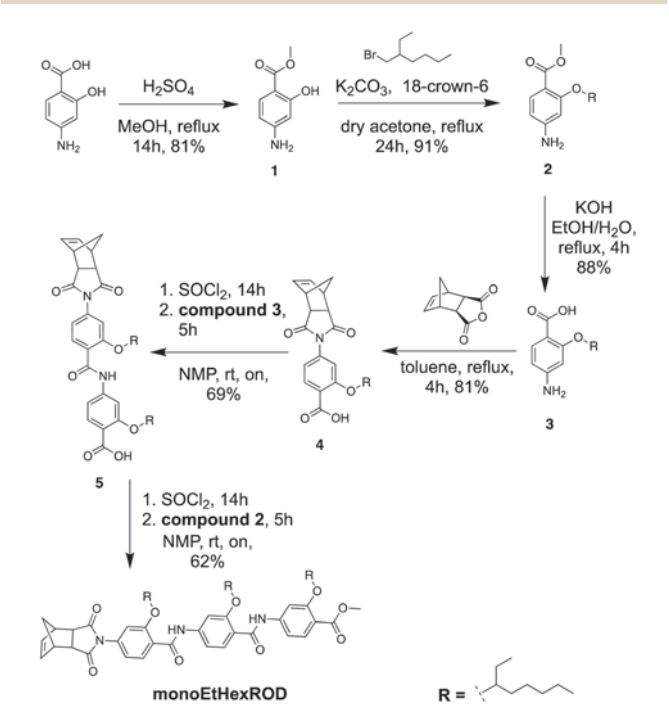

Scheme 1 Multistep synthesis of the ethylhexyl-rod monomer (**monEtHexROD**).

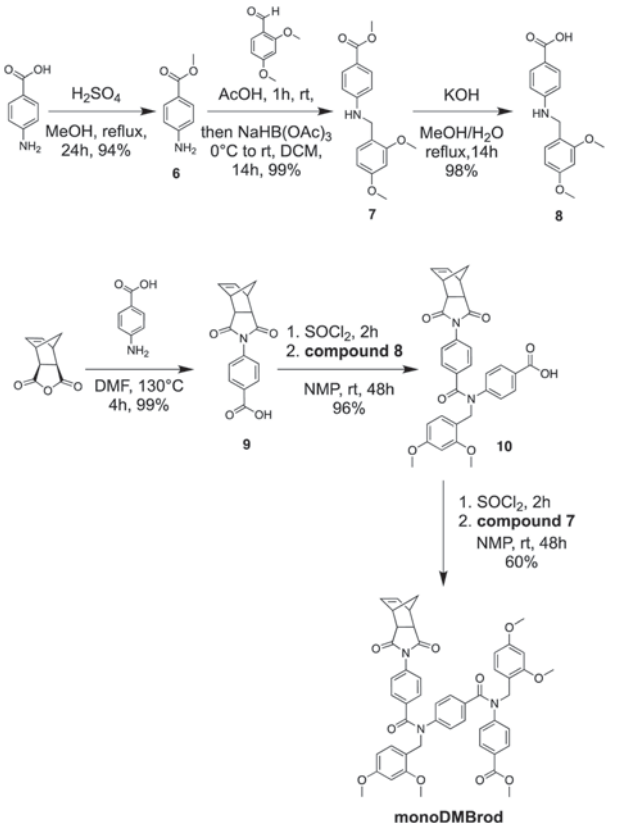

Scheme 2 Multistep synthesis of the DMBrod monomer (**monoDMBrod**).

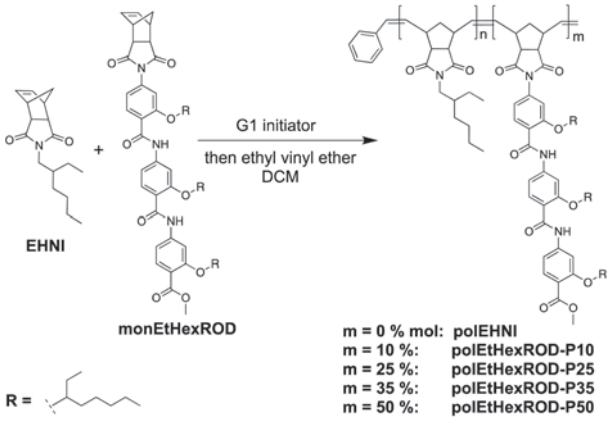

Scheme 3 Synthesis of **polEHNI** and copolymers of **EHNI** and different mol percentages of **monoEtHexROD**.

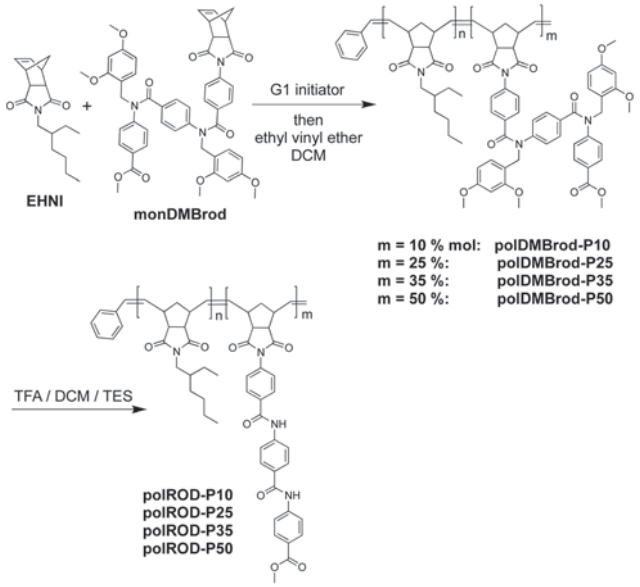

Scheme 4 Synthesis of copolymers containing **EHNI** and different mol percentages of DMB-protected rod monomer and DMB-deprotection of the copolymers.

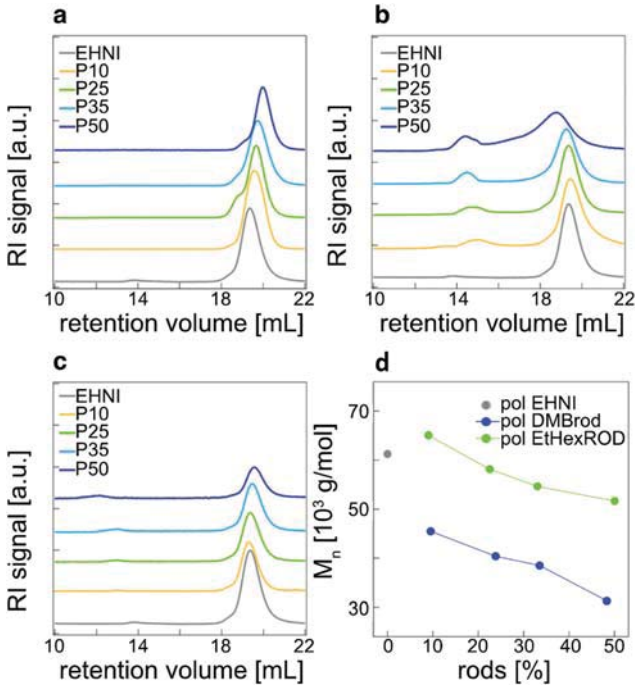

Fig. 1 GPC elution curves (solvent: THF, calibration: polystyrene standards, detector: refractive index) of polymer samples: (a) DMB-protected rods (**polDMBrod**) (b) DMB-deprotected rigid side chains (**polROD**), (c) ethylhexyl ether rod polymers (**polEtHexROD**) and (d) influence of the rod content on the number-average molecular weight. Data of **polEHNI** are also shown.

correspond to **monoEtHexROD** and **monoDMBrod** respectively. Finally, **polROD** corresponds to the deprotected form of **polDMBrod**. A reference polymer with only **EHNI** (**polEHNI**) was also prepared.

Gel Permeation Chromatography/Size Exclusion Chromatography (GPC/SEC) traces of all polymers prepared are shown in Fig. 1. The GPC traces show narrow peaks with molecular weight dispersities between $Đ$ = 1.1 and 1.2 for the reference polymer **polEHNI** and both copolymer series, **polDMBrod** and **polEtHexROD**. However, as can be seen in Fig. 1a and c, the molecular weight decreases with increasing rod content. ^{1}H-NMR data indicates that the desired molar ratio between either **monDMBrod** or **monEtHexROD** and **EHNI** monomer is identical to the monomer feed ratio. This demonstrates that the steric hindrance of the rods might slow down the reaction, but it does not interfere with the relative reactivity of the two monomers. Furthermore, GPC traces for the DMB-deprotected **polROD** polymers show an increase of the molecular weight due to aggregation *via* H-bonds in THF (see Fig. 1b). These measurements are supported by dynamic light scattering (DLS) experiments in THF (Table 1, and Fig. S2†). Both **polDMBrod** and **polEtHexROD** polymers show hydrodynamic radii r_H between 6 and 10 nm, indicating good solvation and no aggregate formation. On the other hand, polymers **polROD-P10** and **polROD-P25** show hydrodynamic radii of 211 and 522 nm, respectively, even at low rod concentration, indicating strong aggregation. For **polROD-P35** and **polROD-P50** DLS was impossible, due to the insolubility of these polymers in THF caused by strong aggregation.

All polymers were further analysed by thermogravimetric analysis (TGA) and differential scanning calorimetry (DSC). Fig. 2a–c show the results of the thermogravimetric analysis of all polymers under nitrogen atmosphere. In general, the TGA traces do not indicate a very significant change in thermal stability, regardless of the copolymer composition, and the decomposition onset temperatures are comparable. No degradation can be detected until 400 °C, even for the **polEHNI** homopolymer. At higher temperatures, a continuous decomposition occurred for all compounds, as expected for random/statistical copolymers.[18] A hypothetical block copolymer for-

http://doc.rero.ch

http://doc.rero.ch

Table 1 Number-average molecular weight (M_n) and dispersity ($Đ$) derived from GPC data (solvent: THF, calibration: polystyrene standards), DLS data (0.5 mg mL^{-1} THF solutions), experimental rod content calculated from NMR integrals, and the glass transition temperature (T_g) established by DSC measurements

Polymer	$M_n \times 10^3$ [g mol^{-1}]	$Đ$	r_H [nm]	Rod [%]	T_g [°C]
polEHNI	61	1.1	10	0	72
polDMBrod-P10	46	1.1	10	9.5	91
polDMBrod-P25	40	1.1	9	23.8	115
polDMBrod-P35	39	1.2	8	33.5	123
polDMBrod-P50	31	1.1	6	48.3	129
polROD-P10	54	1.2	211	—	104
polROD-P25	61	2.6	522	—	147
polROD-P35	100	2.9	N/A	—	171
polROD-P50	218	2.4	N/A	—	201
polEtHexROD-P10	65	1.2	7	9.0	82
polEtHexROD-P25	58	1.2	7	22.5	98
polEtHexROD-P35	55	1.2	7	33.9	106
polEtHexROD-P50	52	1.2	7	50.0	118

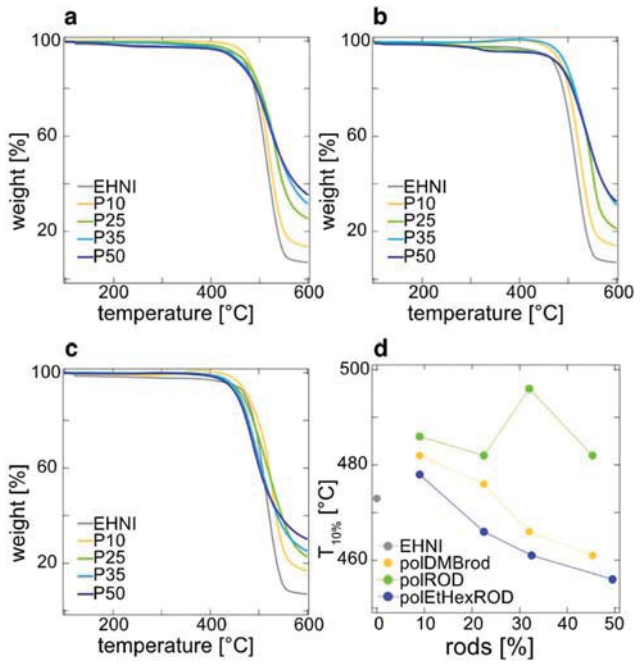

Fig. 2 Thermogravimetric analysis traces of polymer samples: (a) DMB-protected (**polDMBrod**), (b) DMB-deprotected (**polROD**), (c) ethylhexyl ether carrying rod polymers (**polEtHexROD**) and (d) temperatures of 10% weight loss as function of rod content.

mation would be indicated by a step-wise weight loss, which is, however, not observed. Comparing the temperatures at 10% weight loss, $T_{10\%}$, a difference in the decomposition behaviour of the different rods incorporated in the polymer can be observed. The DMB-deprotected **polROD** show the highest $T_{10\%}$ values, followed by the DMB-protected **polDMBrod**, and the lowest temperature $T_{10\%}$ are seen for **polEtHexROD** (Fig. 2d). It has to be noted that the thermostability decreases with the augmentation of the rod concentration for **PolDMBrod** and **polEtHexROD**. This is attributed mainly to the loss of DMB-protecting group and the ethyl hexyl side chain for both polymers respectively.

These results imply that the interactions between rods have a positive influence on thermostability of the material, when hydrogen bonds are present. However, these differences are relatively small due to the fact, that the backbone of **polEHNI** already shows a high thermal stability. TGA data also show an increasing residual mass fraction at 600 °C with higher rod content, indicating that the remaining mass consisted of the more stable aromatic side chains.

To obtain a better understanding of the influence of different rods on the thermal properties of the polymers, DSC measurements were performed. The results are illustrated in the graphs shown in Fig. 3a–c. Since the TGA measurements reveal that all polymers are stable below 300 °C, DSC measurements were performed between −80 °C and 300 °C. Homopolymer **polEHNI** exhibits a glass transition temperature (T_g) of 72 °C. The T_g of the copolymers predominantly depends on the concentration, but also on the nature of the attached rod, and increases to up to 201 °C for the compositions investigated. Plots of T_g *vs.* the rod content (see Fig. 3d) clearly show a linear dependence for both, **polROD** and **polEtHexROD**. The slope of the function, and hence the influence of rod content, is higher for **polROD**. This indicates that H-bonding between the amide groups shows a greater influence on T_g, than dispersion forces between flat rod-like

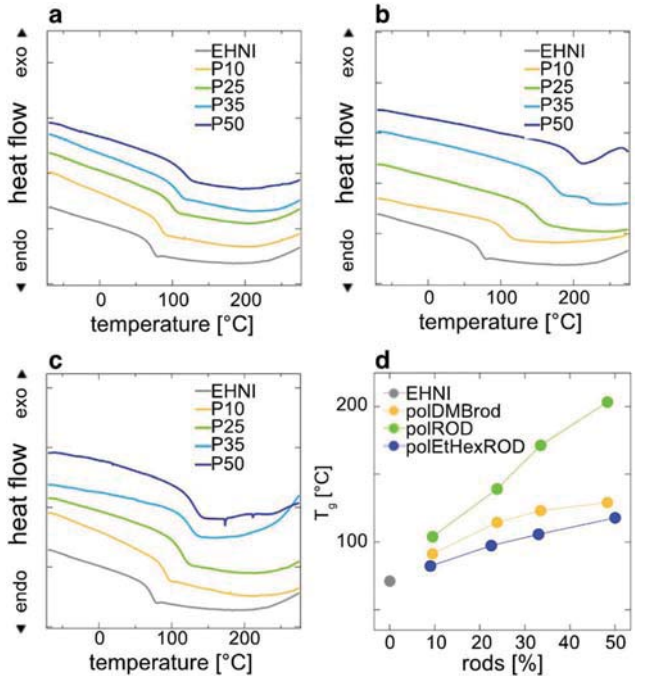

Fig. 3 Traces of the second heating in DSC analysis of polymer samples: (a) DMB-protected (**polDMBrod**), (b) DMB-deprotected (**polROD**) and (c) ethylhexyl ether rod carrying polymers (**polEtHexROD**). Graph (d) is indicating the dependence of T_g on the rod content. For full heating–cooling cycles see Fig. S6.†

molecules in the case of **polEtHexROD**. This behaviour is possibly due to the reduction of internal plasticization.[19] By decreasing the amount of the flexible **EHNI** spacers, the rigid components are closer to each other and hence interactions are more likely to occur. Furthermore, it must be noted, that the increasing molecular weight does not significantly affect the T_g.[20,21]

Annealing the polymers at 15 °C above their respective T_g did not affect the T_g for **polROD** samples (Fig. S7†). Furthermore, annealing did not lead to crystallization, confirming the expectation that these copolymers are fully amorphous.[22] One can speculate that an increase of the rod content would lead to a further increase of T_g. However, higher percentages of the rigid side chains would most likely also lead to insolubility and such compositions were thus not investigated.

After investigation of the thermal characteristics, attention was paid to the mechanical properties of the polymers. For this purpose, polymer films were produced by compression molding in a hot-press. Films with a thickness of 0.12 mm ± 0.01 mm were produced. Unfortunately, films made from polymers with a rod-content of more than 10% proved to be too brittle to handle. Thus, only the mechanical properties of **polEHNI**, **polDMBrod-P10**, **polROD-P10**, and **polEtHexROD-P10** could be compared. ESI Fig. S8 and S9† show the stress–strain curves and Table 2 lists the maximum stress (σ_{max}), elongation at maximal stress (ε), the Young's moduli (E) and the storage modulus (E') of the respective polymers.

All polymers tested display ultimately very similar mechanical properties. An elongation at maximal force of the order of 3% is observed for all polymers. Some of the stress–strain curves appear to show some yielding (ESI Fig. S9†), and the maximum strain at break was in all cases lower than 20%. Unfortunately, perhaps due to sample inhomogenities, the tensile test results show considerable variations (ESI Fig. S9†), and no clear trend with respect to the elongation at break could be established. On the other hand, the introduction of the aramids appears to lead to a slight increase of the tensile strength σ_{max}. Indeed, amongst all samples investigated, **polROD-P10** showed the highest σ_{max}, which is attributed to H-bonding effecting the tensile strength beneficially compared to **polEHNI**. For **polEtHexROD-P10** a decrease of σ_{max} was observed, indicating that **monEtHexROD** were not able to interact *via* H-bonds but rather disturb the internal structure of the backbone. **polDMBrod** and **polROD** also display the highest Young's moduli (1.5 and 1.6 GPa, respectively), but again, the differences between the compositions are very small.

To get an insight into the thermal dependence of the mechanical properties, temperature dependent dynamic mechanical analysis (DMA) experiments were conducted. The DMA traces (Fig. 4) reveal a rigid, glassy regime, with a room-temperature storage modulus E' that increases from 1.3 GPa (**polEHNI**) to 1.6 GPa for **polROD-P10** This is clearly indicating the beneficial effect of H-bonds on the E' modulus. For **polDMBrod** and **polEtHexROD** no improved storage moduli were obtained, as indicated by similar DMA traces as for **polEHNI**. The DMA traces also clearly confirm an increase of the T_g, which increases from 72 °C (**polEHNI**) to 82 °C (**polEtHexROD-P10**) to 91 °C (**polDMBrod-P10**) to 104 °C **polROD-P10**. Thus, the DMA data confirm the DSC results and indicate that the introduction of H-bonding monomers has the largest influence on T_g.

Powder X-ray diffraction (XRD) experiments were performed, in order to get insight in the molecular organization of the side chains within the polymer. Diffraction patterns are shown in Fig. 5. For **polEHNI** two diffuse scattering halos at 2θ = 5° and 2θ = 17.5° are present. Even though these broad, diffuse peaks show some degree of organization, the absence of sharp Bragg peaks reveals that **polEHNI** shows no crystallinity. Upon increasing the rod content in both series, **polEtHexROD** and **polROD**, an incremental decrease of the intensity of the diffuse peaks was observed. This effect was attributed to the interference of the bulky rod side chains with

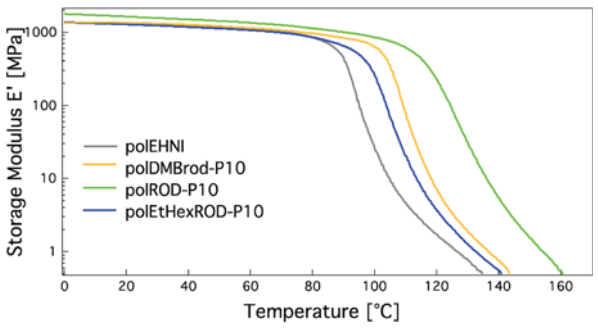

Fig. 4 Temperature dependence of storage modulus E' obtained *via* DMA experiments on 0.12 ± 0.01 mm hot-pressed films of polymer samples.

Table 2 Mechanical properties determined *via* different DMA experiment of all compositions suitable for mechanical analysis (higher rod-content polymers were to brittle)

Polymer	Tensile strength σ_{max} [MPa]	Elongation at maximal stress ε_{max} [%]	Young's modulus E [GPa]	Storage modulus E' (25 °C) [GPa]
polEHNI	31	3.3	1.3	1.3
polDMBrod-P10	34	3.1	1.6	1.2
polROD-P10	37	3.0	1.5	1.6
polEtHexROD-P10	26	2.7	1.2	1.2

http://doc.rero.ch

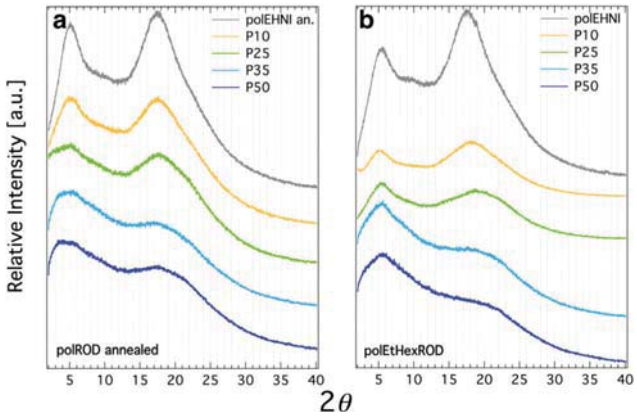

Fig. 5 Powder X-ray diffraction profiles at 25 °C for different rod containing samples: (a) **polROD** annealed 15 °C above their respective T_g and (b) ethylhexyl rod carrying polymers **polEtHexROD**. Graphs presented with intensity offset for clarity.

the organization of ethylhexyl side groups in **polEHNI** and the related spacing of the backbone. It must be noted, that annealing at 15 °C above T_g of **polROD** samples was necessary in order to observe this trend. Based on X-ray diffraction data, it can be concluded, that all different polymers show amorphous behaviour.

Interestingly, even though **polEHNI** did not show real crystallinity, some birefringence was observed by cross-polarized light microscopy due to organization of the backbone to some extent (POM, ESI Fig. S12†). Also, the POM images of precipitated copolymers show some birefringence, which, however, decreased with increasing rod content (Fig. S11–S13†). In order to investigate if the rod-like side chains may serve as mesogens and if polymers with higher rod content would show liquid crystalline behaviour at elevated temperatures, POM was also performed under heating the samples (to 15 °C above their respective T_g). However, heating the polymers extinguished the birefringence entirely, as shown in ESI Fig. S11–S13.† The same result was observed, when high-rod-content polymers **polROD-P35** and **polROD-P50** were annealed 15 °C above their respective T_g and cooled down very slowly (ESI Fig. S13.† Additionally, DSC curves of these samples showed no exothermic peaks, indicating no crystalline behaviour (ESI Fig. S7†). In summary, all observations made by means of POM support X-ray measurements. Initial organization (not crystallinity) of **polEHNI** was inhibited by introduction of rigid rod side groups into the polymers.

Conclusion

Two series of new comb-like poly(norbornene)s carrying lateral rod-like aramid group were synthesized in which the aramid moieties display different types of non-covalent interactions. The results show that the glass transition temperature increases proportionally with the concentration of the H-bonding monomer. All polymers showed a T_g above room temperature, which renders the materials glassy and brittle. The high T_g also provides a high stiffness and high temperature stability. It was found, that the brittleness of the material increases with increasing rod content; in fact, materials with a rod content of higher than 10% were too brittle for mechanical analysis. DSC analyses indicated that all polymers are amorphous, which is supported by X-ray diffraction before and after annealing. Investigations of their material properties showed an increasing T_g due to the H-bond interaction between the aramid rods and a linear increase of T_g proportionally to the rod percentage. Hence, DMB-deprotected rod polymers showed overall the highest T_g according to their rod percentages. This means the hydrogen bond interaction within the polymer are stronger than the π–π-stacking carried by EtHexROD polymers as expected. High T_g polymers are of interest due to their thermal stability. However, most of these materials are difficult to handle due to the heat required to be processed. These rod-containing polymers are interesting because they could be processed in solution at lower temperature than their respective T_g. These results showed that aramid rods could be used for the synthesis of polymers with tailor-made thermal behaviour as it is the case for heat resistant and/or fire-retardant materials.

Conflicts of interest

There are no conflicts to declare.

Acknowledgements

PK, SD, SS, CW and AFMK thank the National Center for Competence in Research (NCCR) "Bio-inspired Materials" and the Swiss National Science Foundation for financial support. Furthermore, the authors thank the following people for support: Worarin Meesorn (DMA experiments, Adolphe Merkle Institute), Aurelién Crochet (powder X-ray, University of Fribourg) and Sandra Graterol (DSC, Adolphe Merkle Institute).

Notes and references

1 P. W. Morgan, *Macromolecules*, 1977, **10**, 1381–1390.
2 M. G. Northolt and J. J. van Aartsen, *J. Polym. Sci., Polym. Lett. Ed.*, 1973, **11**, 333–337.
3 M. G. Northolt, *Eur. Polym. J.*, 1974, **10**, 799–804.
4 D. Tanner, J. A. Fitzgerald and B. R. Phillips, *Angew. Chem., Int. Ed. Engl.*, 1989, **28**, 649–654.
5 H. Seyler, E. Berger-Nicoletti and A. F. M. Kilbinger, *J. Mater. Chem.*, 2007, **17**, 1954–1957.
6 M. Schulze, B. Michen, A. Fink and A. F. M. Kilbinger, *Macromolecules*, 2013, **46**, 5520–5530.
7 H. Seyler and A. F. M. Kilbinger, *Macromolecules*, 2009, **42**, 9141–9146.

http://doc.rero.ch

8 H. Seyler and A. F. M. Kilbinger, *Macromolecules*, 2010, **43**, 5659–5664.
9 V. Shibaev, A. Bobrovsky and N. Boiko, *Prog. Polym. Sci.*, 2003, **28**, 729–836.
10 K. O. Kim and T. L. Choi, *ACS Macro Lett.*, 2012, **1**, 445–448.
11 M. Saariaho, A. Subbotin, I. Szleifer, O. Ikkala and G. Ten Brinke, *Macromolecules*, 1999, **32**, 4439–4443.
12 T. Kato, J. Uchida, T. Ichikawa and B. Soberats, *Polym. J.*, 2018, **50**, 149–166.
13 Y. F. Zhu, Z. Y. Zhang, Q. K. Zhang, P. P. Hou, D. Z. Hao, Y. Y. Qiao, Z. Shen, X. H. Fan and Q. F. Zhou, *Macromolecules*, 2014, **47**, 2803–2810.
14 Y. Zhang, R. Cao, J. Shen, C. S. F. Detchou, Y. Zhong, H. Wang, S. Zou, Q. Huang, C. Lian, Q. Wang, J. Zhu and B. Gong, *Org. Lett.*, 2018, **20**, 1555–1558.
15 C. A. Hunter and J. K. M. Sanders, *J. Am. Chem. Soc.*, 1990, **112**, 5525–5534.
16 C. A. Hunter, K. R. Lawson, J. Perkins and C. J. Urch, *J. Chem. Soc., Perkin Trans. 2*, 2001, **5**, 651–669.
17 C. R. Martinez and B. L. Iverson, *Chem. Sci.*, 2012, **3**, 2191–2201.
18 C. De Ruijter, W. F. Jager, J. Groenewold and S. J. Picken, *Macromolecules*, 2006, **39**, 3824–3829.
19 T. Hu, J. Yi, J. Xiao and H. Zhang, *Polym. J.*, 2010, **42**, 752–758.
20 T. G. Fox and P. J. Flory, *J. Polym. Sci.*, 1954, **14**, 315–319.
21 Z. Komiya, C. Pugh and R. R. Schrock, *Macromolecules*, 1992, **25**, 3609–3616.
22 G. Mao, J. Wang, S. R. Clingman, C. K. Ober, J. T. Chen and E. L. Thomas, *Macromolecules*, 1997, **30**, 2556–2567.

http://doc.rero.ch